ORIGINAL ARTICLE

DOI: https://doi.org/10.18599/grs.2020.3.48-54

Russian Original 2020. Vol. 22. Is. 3. Pp. 48–54

Vosnesensky Cu-porphyry deposit (Southern Urals): formation conditions, trace elements, sulfur isotopes and fluid sources

S.E. Znamensky[1], N.N. Ankusheva[2], D.A. Artemiev[2]*

[1]*Institute of Geology of the Ufa Federal Research Centre of the Russian Academy of Sciences, Ufa, Russian Federation*

[2]*Institute of Mineralogy of the South Urals Federal Research Center of Mineralogy and Geoecology of the Urals Branch of the Russian Academy of Sciences, Miass, Russian Federation*

Abstract. The paper shows new fluid inclusion and isotopic-geochemical data for minerals from sulphide-carbonate-quartz veins of Vosnesensky Cu-porphyry deposit. Fluid inclusions were analyzed by means Linkam TMS-600 cryostage equipped with Olympus BX 51 optical microscope; trace element amounts were performed used Agilent 7700x and ELAN 9000 mass-spectrometers; sulphur isotopic composition was analyzed on DeltaPLUS Advantage mass-spectrometer. We determined that fluid inclusions in quartz were homogenized between 215 and 315ºC, and in latest calcite, they are 230–280ºC. Fluids are K-Na water chloride with salinity of 3–12 wt % NaCl-eq. Quartz contain high amounts of Al (184–5180 ppm), K (20.1–1040 ppm), Na (30.2–1570 ppm) and Ti (38.4–193 ppm). The REE distribution spectra of pyrite are characterized by light lanthanides accumulation (LaN/YbN = 3.6–6.44), and negative of Ce anomalies (0.7–0.92) and Eu (0.78–0.99). The Y/Ho ratio in pyrite varies from 27.6 up to 36.8. The $\delta^{34}S$ values in pyrite were –1.01…0.8 ‰, in chalcopyrite – 0.9 ‰. The data testify the Cu-porphyry mineralization of Vosnesensky deposit was formed due to magmatic acid high-aluminous K-Na chloride fluid enriched with light REE in mesothermal environment. We identified the geochemical markers of interaction between fluid and host rocks.

Keywords: Southern Urals, Cu-porphyry deposit, fluid inclusions, trace elements, LA-ICP-MS, sulphur isotopic composition

Recommended citation: Znamensky S.E., Ankusheva N.N., Artemiev D.A. (2020). Vosnesensky Cu-porphyry deposit (Southern Urals): formation conditions, trace elements, sulfur isotopes and fluid sources. *Georesursy = Georesources*, 22(3), pp. 48–54. DOI: https://doi.org/10.18599/grs.2020.3.48-54

Introduction

The Vosnesensky Cu-porphyry deposit is located in the Main Ural Fault zone in the Southern Urals. Cu-porphyry mineralization, which until recently was considered atypical for the Urals, is beginning to acquire more and more economic importance. In recent years, several large Cu-porphyry deposits have been discovered only in the Southern Urals, some of which are already being mined or prepared for exploitation (Mikheevsky, Severo-Tominsky, etc.). At the same time, the degree of knowledge of the formation conditions and genetic characteristics of the porphyry family in the Urals remains insufficient. This also applies to the Vosnesensky deposit, which by many researchers belongs to the reference Cu-porphyry objects associated with island arc diorite magmatism (Grabezhev, 2009; Seravkin et al., 2011). Thanks to the works of V.B. Shishakov et al. (Shishakov et al., 1988), A.I. Grabezhev and E.A. Belgorodsky (Grabezhev, Belgorodsky, 1992), A.M. Kosarev et al. (Kosarev et al., 2014), S.E. Znamensky et al. (Znamensky et al., 2019), the structure, petrological and geochemical characteristics of the ore-hosting rocks, the structure and composition of the near-ore aureole of the deposit were studied. In order to clarify the conditions for the Cu-porphyry mineralization formation and the nature of the mineral-forming fluid, for the first time we carried out thermobarogeochemical studies, determined the concentrations of trace elements and isotopic ratios of S in ore minerals.

Geological background

The Vosnesensky deposit is located at the northern end of the massif of the same name, in the structure of which hornblende gabbro-diorites, diorites and, in some places, granodiorites (Figure 1). The U-Pb age of zircons from the diorites of the massif is 412±3 Ma (Kosarev et al., 2014). The massif occurs in serpentinite melange containing blocks of serpentinite-clastic breccias, pyroxenites, diabases, basalts and silica of unknown age, as well as Lower Devonian organogenic limestones.

Stringer sulfide-carbonate-quartz mineralization (Figure 2) is spatially closely related to dikes of quartz-

*Corresponding author: Sergey E. Znamensky
E-mail: Znamensky_Sergey@mail.ru

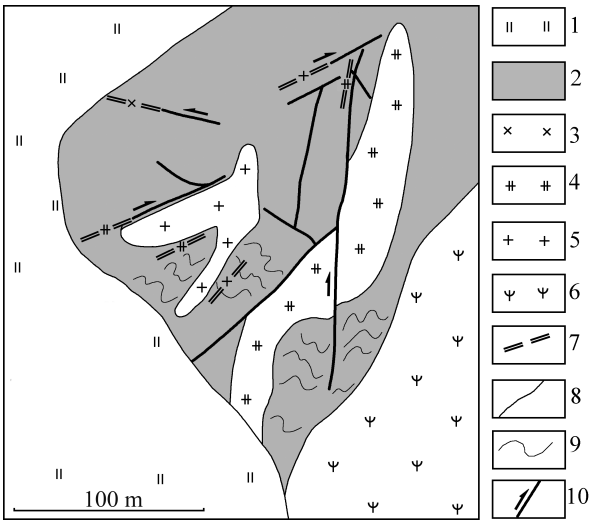

Fig. 1. Geological and structural scheme of the Vosnesensky deposit (Znamensky et al., 2019). 1 – Quaternary sediments; 2 – hornblende gabbro-diorites, diorites and granodiorites of the Vosnesensky massif; 3–5 – dike series: 3 – diorite-porphyrites, 4 – granodiorite-porphyry, 5 – plagiogranite-porphyry, 6 – serpentinite, 7 – dikes (shown outside the scale); 8 – geological boundaries; 9 – banding in the dioritoids of the Vosnesensky massif; 10 – magma-ore-controlling faults (arrows indicate the direction of displacement of the wings).

Fig. 2. Stringer pyrite-chalcopyrite-carbonate-quartz ore mineral

bearing diorite-porphyrites, granodiorite-porphyry, and plagiogranite-porphyry (Znamensky et al., 2019). All types of granitoids are characterized by porphyry precipitates of plagioclase and hornblende. In the host rocks of the Vosnesensky massif, the intensity of mineralization decreases. The placement of dikes is controlled by faults of near-meridional, northwestern and northeastern striking, forming a zone of right strike slip within the massif. Ore-hosting granitoids belong to the island arc calc-alkaline magmatites of normal alkalinity. Geochemically, they are close to the rocks of the Vosnesensky massif and, apparently, represent its late "porphyry" phase (Znamensky et al., 2019).

Pyrite and chalcopyrite are the main ore minerals in stringer sulfide-carbonate-quartz ores. Sphalerite, pyrrhotite, and molybdenite are found sporadically. According to V.B. Shishakov et al. (Shishakov et al., 1988), molybdenite is present in the form of scattered dusty in rare quartz veins and only in some cases forms single radial-radiant aggregates 0.3–1.0 mm in size in these veinlets. Molybdenite mineralization has no practical value. The total content of sulfides in the total mass of ore usually does not exceed 2–3%. According to its optical properties and thermal analysis data, carbonate in ores is represented by calcite. Near-ore metasomatites have sericite-quartz or sericite-quartz-chlorite composition, often with an admixture of carbonate. The metasomatites of individual dikes contain biotite and potassium feldspar in association with magnetite. At a distance from the ore halo, the rocks of the Vosnesensky massif underwent propylite alteration of the chlorite-epidote and actinolite-epidote facies.

Analytical methods and results

Fluid inclusions

Fluid inclusions in quartz and later calcite of stockwork ores were studied. The studies were carried out in the laboratory of thermobarogeochemistry of the South Ural State University (Miass, analyst N.N. Ankusheva). Thermometric measurements were carried out in a TMS-600 cryostage (Linkam) with LinkSystem 32 DV-NC software and an Olympus BX51 optical microscope. The interpretation of the eutectic temperatures of fluids in inclusions was carried out using the work (Davis et al., 1990). The salinities of fluids in inclusions were determined from the final melting temperatures of ice in inclusions according to (Bodnar, Vityk 1994). The homogenization temperatures of the inclusions are taken as the minimum temperatures of mineral formation (Roedder, 1984). The processing of the results was performed using the Statistica 12 program. The results are shown for 140 inclusions.

Quartz in ore veins forms large grains. The mineral is translucent to milky white, medium-grained. It contains syngenetic two-phase inclusions 10–15 μm in size (Figure 3a, 2). Gas vacuoles occupy up to 15–20% of their volume. The inclusions have an oval, angular shape, sometimes with small processes and/or with elements of crystallographic facets and are evenly distributed, occur both singly and in groups of 2–3 inclusions.

For inclusions, eutectic temperatures equal to –21 ... –24°C and temperatures of the end of ice melting – –8.3 ... –3.7°C were obtained. These data correspond to a chloride fluid containing K and Na ions with a concentration of 4.8–12 wt. % NaCl-eq. with a mode of 8–9 wt. % (Figure 3b). Homogenization temperatures (into liquid) were 215–315°C with a polymodal distribution of values (Figure 3c).

Calcite forms semitransparent grains with weak birefringence and cryptocrystalline aggregates and veinlets cutting through quartz. It also analyzed

syngenetic two-phase inclusions (Figure 3a, 1). They are 8–15 μm in size, isometric or sinuous in shape, are located singly, gas vacuoles in them are medium-sized, occupy about 15% of the inclusion volume.

The eutectic temperatures of solutions in inclusions, varying from –21 to –23°C, indicate the content of Na and K chlorides in the fluid. Salt concentrations, according to ice melting points ($T_{m.}$ = –4 ... –2°C), are 3–10 wt. % NaCl-eq. with a bimodal distribution of values and unexpressed modes of 3–4 and 7–8 wt. % (Figure 3b). The temperatures of homogenization into the liquid phase were 230–280°C with peaks at 240–250 and 260–270°C (Figure 3c).

The values of the homogenization temperatures and fluid salinity in inclusions in both quartz and calcite are characterized by a weak positive correlation (Figure 3d). Most inclusions in quartz and calcite are characterized by similar parameters and salinity, but more highly concentrated inclusions in quartz and low-salinity inclusions in calcite are distinguished. This may indicate the deposition of both minerals as a result of the evolution (cooling) of a fluid of the same composition and genesis.

In calcite and quartz, secondary two-phase inclusions with sizes of the first micrometers, tracing cracks in minerals, were also studied (Figure 3a). Salt concentrations of 1.5–1.9 wt.% were obtained for them. % NaCl-eq. ($T_{m.}$ = –0.9 ... –1.1°C) and homogenization temperatures (into liquid) equal to 110–120°C (Figure 3a). In addition, a large number of single-phase inclusions with the size of the first micrometers, located around two-phase syngenetic inclusions, are recorded.

Trace elements in quartz

The concentrations of trace elements in quartz were determined by the method of laser ablation with inductively coupled plasma on an Agilent 7700x mass spectrometer with the MassHunter software package and a New Wave Research UP-213 laser sampler at the Institute of Mineralogy of the SU FRC MG UB RAS (Miass, analyst D.A. Artemiev).

The main trace elements in quartz are: Al (184–5180 ppm), K (20.1–1040 ppm), Na (30.2–1570 ppm), and Ti (38.4–193 ppm) (Table 1), which are most often included in its structure and depend on the conditions of formation. Li, Mg, P, Ca, Sc, and Fe are also found in high concentrations. The Al content in the quartz lattice, which depends on the pH of the fluid, varies within the range 184–750 ppm (on average, 440 ppm). In some cases, an increase in its content to 5180 ppm is noted, which, along with increased concentrations of Na, K, and Ca, indicates that feldspar microinclusions (points B-9-10 and B-9-11) have entered the ablation area. The Ti content is in the range 38.4–193 ppm (121 ppm on average) and depends on the temperatures of quartz formation. Lithium (1.2–7 ppm), K (20.1–212 ppm), Mg (4.4–49 ppm), and Na (30.2–174 ppm) can enter in small amounts in the crystal lattice of quartz, but usually, their increased concentrations are associated with fluid inclusions containing chlorides in the liquid phase. So, at point B-9-7, the sodium content differs sharply from the neighboring points, due to inclusions in the ablation zone. The Ca content varies within the range of 47.7–108 ppm; higher concentrations may be associated with microinclusions of calcite and feldspars in quartz veins (points B-9-10 and B-9-11). Normal Fe concentrations for the Vosnesensky quartz deposit are in the range of 3.3–10.9 ppm (on average, 5.4 ppm). Higher grades, up to 67 ppm, are likely associated with microinclusions of carbonates (point B-9-8) and feldspars (points B-9-10 and B-9-11). The contents of P and Sc are homogeneous, but can only serve as informative values, since in silicon-

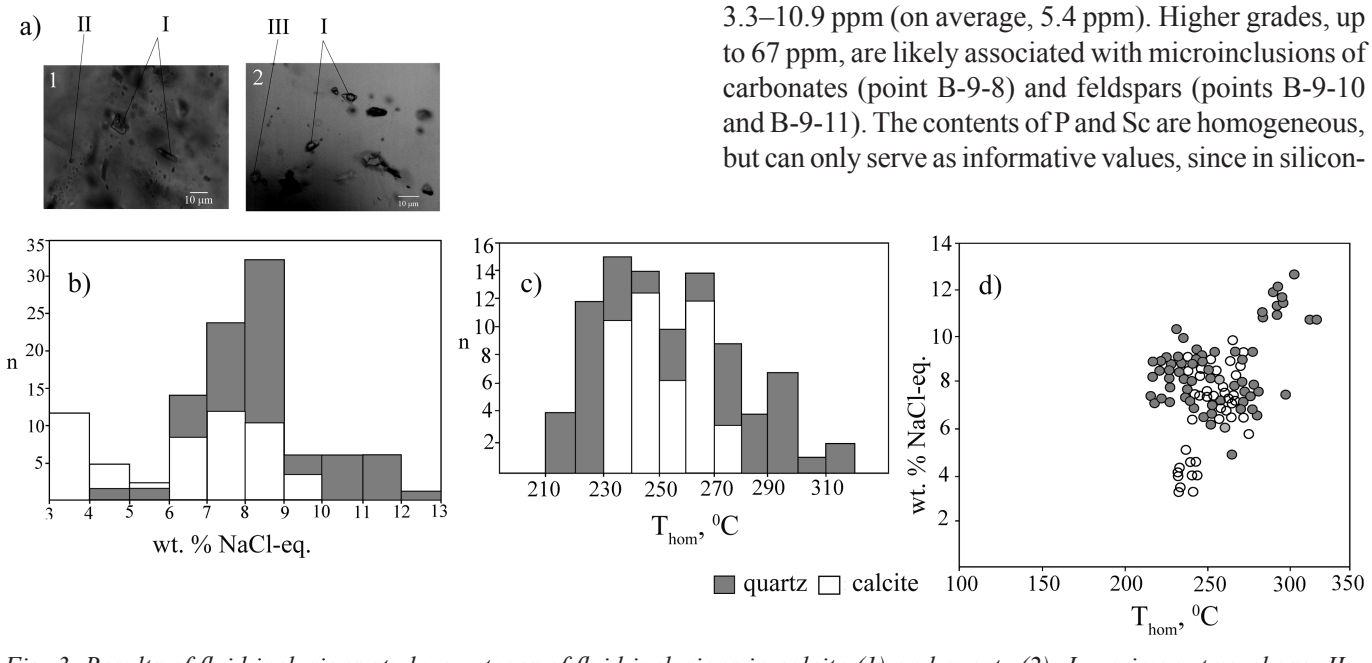

Fig. 3. Results of fluid inclusions study. a – types of fluid inclusions in calcite (1) and quartz (2): I – primary two-phase; II – secondary two-phase; III – single phase. b, c – distribution of salinity (b) and homogenization temperatures (d); n is the number of measurements; d – ratio of salinity and homogenization temperatures of inclusions.

Element/ sample	Li	Na	Mg	Al	P	K	Ca	Sc	Ti	Fe
B-6-1	6.09	71	21.5	184	40	20.1	108	14.23	166	6.7
B-6-2	5.3	30.2	23.19	527	29.2	160.4	47.7	12.89	193	5.37
B-6-3	4.79	44.8	16.28	384	30.5	109.2	61.8	12.37	117	3.49
B-6-4	4.47	35	21.6	471	31.4	174.1	55	12.03	167	5.65
B-6-5	5.59	59.5	23.05	557	38.8	141.7	60.8	11.43	164	5.29
B-6-6	7	33.1	21.4	450	33	186	74	11.3	168	6.8
B-6-7	5.15	47.41	23	516	42.7	162.9	75.9	10.43	159	5.69
B-6-8	4.25	45	9.23	259	40.7	56.9	84.6	10.12	146	3.28
B-6-9	5.01	36.3	25.25	539	37.6	186.6	60	9.94	177	6.65
B-9-1	3.99	66.7	6.66	202	29.1	52.5	94	9.59	146	2.46
B-9-2	2.92	53.7	4.38	245	34.1	70.8	79	8.65	58.9	1.09
B-9-3	2.75	76.6	19.69	400	31.9	132	67.5	8.46	76.3	10.88
B-9-4	4.78	42.8	17.8	522	40.2	186.5	85	8.09	78.4	6.54
B-9-5	1.23	44.5	4.87	261	40	84.5	101	8.16	38.4	1.5
B-9-6	2.74	48	10.64	426	44.5	132.8	77	8.06	62.3	7.61
B-9-7	4.02	174	17.1	620	44	134.6	56.7	7.77	134	6.18
B-9-8	1.23	47.73	49	750	49.8	158	123	7.85	59	36
B-9-9	3.07	57.9	11.7	588	46.6	212	145	7.63	76.6	6.3
B-9-10	3.57	72	35	1370	46.4	532	131	7.58	86.4	20.7
B-9-11	1.94	1570	124	5180	55.3	1040	350	7.34	88	66.7

Table 1. Content of trace elements in quartz, ppm

oxygen compounds in mass spectrometry, interference overlaps of ^{31}P with $^{30}Si+H$ or $^{14}N+^{16}O+H$ and others are observed, and ^{45}Sc – with $^{29}Si+^{16}O$ or $^{28}Si+^{17}O$.

Distribution of rare earth elements and yttrium in ore pyrite

The contents of rare earth elements and yttrium in pyrite were determined by inductively coupled plasma mass spectrometry (ICP-MS) on a PerkinElmer ELAN 9000 instrument at the Institute of Geology and Geochemistry of the Ural Branch of the Russian Academy of Sciences (Yekaterinburg, analyst D.V. Kiseleva). The standardization was carried out for CI chondrite (McDonough, Sun, 1995). The Eu and Ce anomalies were calculated using the formulas:

$Eu/Eu^* = Eu_N/(Sm_N/(Tb_N \times Eu_N)^{0,5})^{0,5}$,

$Ce/Ce^* = Ce_N/((2La_N + Sm_N)/3)$.

The results of the determinations are shown in Table 2.

Sulfur isotopic composition of sulfides

Stable sulfur isotopes have been studied in pyrite and chalcopyrite ores (Table 3). The sulfur isotopic composition was determined on a DeltaPLUS Advantage mass spectrometer coupled with an EA Flash 1112 elementary analyzer and a ConFlo IIII interface at the Institute of Mineralogy of the SU FRC MG UB RAS (Miass, analyst S.A. Sadykov). The error in determining δ34S was 0.27 ‰. The measurement results are given in relation to the international CDT standard. According to the data obtained, the δ34S values in pyrite are – 1.01… 0.8 ‰, in chalcopyrite – 0.9 ‰.

Element/ sample	B3-7	B3-9	B3-12	B3-11	B3-14	B3-13
La	1.1	0.5	1.7	0.7	1.3	0.6
Ce	1.9	1	2.45	1.35	2.1	0.9
Pr	0.16	0.11	0.23	0.14	0.21	0.12
Nd	0.65	0.47	0.76	0.52	0.63	0.43
Sm	0.17	0.1	0.19	0.14	0.16	0.1
Eu	0.056	0.025	0.062	0.04	0.05	0.03
Gd	0.2	0.12	0.25	0.17	0.21	0.13
Tb	0.03	0.03	0.04	0.023	0.03	0.02
Dy	0.24	0.14	0.28	0.18	0.24	0.16
Ho	0.05	0.029	0.06	0.04	0.05	0.031
Er	0.16	0.09	0.18	0.12	0.15	0.08
Tm	0.024	0.013	0.029	0.02	0.024	0.011
Yb	0.17	0.1	0.19	0.14	0.16	0.08
Lu	0.027	0.015	0.031	0.021	0.023	0.012
Y	1.6	0.8	2.21	1.33	1.45	1.13
∑REE	4.94	2.73	6.45	3.6	5.34	2.7
La_N/Yb_N	4.66	3.6	6.44	3.6	5.85	5.39
La_N/Sm_N	4.18	3.23	5.78	3.23	5.25	3.87
Gd_N/Yb_N	0.97	0.99	1.09	1.0	1.09	1.34
Eu/Eu*	0.99	0.78	0.95	0.9	0.93	0.9
Ce/Ce*	0.82	0.92	0.7	0.9	0.78	0.71
Y/Ho	32	27.6	36.8	33.3	29.2	36.5

Table 2. Content of rare earth elements and yttrium in pyrite, ppm

Discussion and conclusion

According to the data of fluid inclusion study, ore quartz of the Vosnesensky deposit was formed at temperatures not less than 215–315ºC, and calcite was deposited later at 230–280ºC. The mineral-forming fluid is characterized by salinity, which in inclusions of quartz varies from 4.8 to 12 wt. % NaCl-eq., in calcite – from 3 to 10 wt. % NaCl-eq. Crystallization of quartz and

No.	Sample	Isotopic composition of sulfur $\delta^{34}S$ ‰, CDT	Comment
1	В3-7п	0.72	pyrite
2	В3-8п	-1.01	pyrite
3	В3-9п	-0.07	pyrite
4	В3-11п	-0.08	pyrite
5	В3-12п	-0.06	pyrite
6	В3-14п	0.80	pyrite
7	В3-17х	0.90	chalcopyrite
8	В3-19п	0.04	pyrite

Table 3. Isotopic composition of sulfur in sulfides

calcite occurred from K-Na aqueous chloride fluid. The obtained temperature values correspond to the conditions of mesothermal sericite-quartz metasomatism, which ore-bearing granitoids underwent. In general, they are comparable with the results of studying the temperature regime of the formation of Cu-porphyry mineralization in sericite-quartz metasomatites of many other porphyry deposits of the Southern Urals associated with island arc diorites magmatism (Grabezhev, 2009). For example, at the Mikheevsky deposit, the Cu-Mo porphyry mineralization was formed at temperatures of 250–300ºC (Abramova et al., 2016).

The coexistence of single-phase gas, liquid and more concentrated two-phase inclusions indicates fluid heterogenization (Prokofiev et al., 1994 and references therein), considered the homogenization temperatures of inclusions as real fluid temperatures during mineral formation. In turn, the presence of a heterogeneous fluid consisting of a concentrated water fluid in equilibrium with the gas phase indicates the boiling in the environment of pressure reduction.

Using the highly sensitive LA-ICP-MS method, which was first used in the study of quartz from porphyry copper deposits in the Southern Urals, it was found that the Vosnesensky quartz deposit is characterized by high contents of Al (184–5180 ppm) and Ti (38.4–193 g/t). The Al concentration in quartz reflects the solubility of this element in the mineral-forming fluid, which largely depends on the pH of the fluid (Rusk et al., 2008). At relatively low temperatures (<500ºC), the Al concentration in quartz is related to the pH of the fluid by an inverse correlation dependence. The results indicate that the quartz of the Vosnesensky deposit crystallized from a high-alumina acidic fluid.

In terms of the quantitative ratio of Al and Ti in quartz, the Vosnesensky deposit is comparable to other Cu-porphyry deposits in the world. The Al-Ti diagram proposed by B.G. Rusk (Rusk, 2012) to separate epithermal, mesothermal orogenic and porphyry deposits according to this indicator, the points of quartz composition of the Vosnesensky deposit fall into the quartz deposit of porphyry deposits or are grouped around this deposit (Figure 4). We also determined the contents of REE and Y, close to them in chemical properties, in the ore pyrite of the deposit. Studies in recent years have shown (Znamensky, 2017; Rimskaya-Korsakova, Dubinin, 2003; Guangzhou et al., 2009; etc.) that the compositions of REE and Y in sulfides inherit the composition of the fluid from which they crystallize and can serve as an indicator of its physical and chemical parameters and source. Lanthanides and yttrium are concentrated in sulfides in crystal lattice defects and in fluid inclusions. In addition, heavy REEs can enter the crystal lattice of sulfides, while light lanthanides can be sorbed on their surface in the form of free ions and, possibly, in the form of hydroxo complexes (Rimskaya-Korsakova, Dubinin, 2003).

The ore pyrite of the Vosnesensky deposit has low REE (∑REE = 2.7–6.45 ppm) and Y (0.8–2.21 ppm) contents. The REE distribution spectra are enriched in light lanthanides (LaN/YbN = 3.6–6.44), which is typical of minerals crystallizing from acidic fluids with a low content of complexing ligands (Schwim, Markl, 2005), as well as small negative anomalies Eu (Eu/Eu* = 0.78–0.99) and Ce (Ce/Ce* = 0.7–0.92) (Figure 5). Differentiation within heavy lanthanides is not pronounced (GdN/YbN = 0.97–1.34).

The redox potential of Eu in aqueous solutions depends on a number of factors and mainly on temperature (Sverjensky, 1984). Negative Eu anomalies

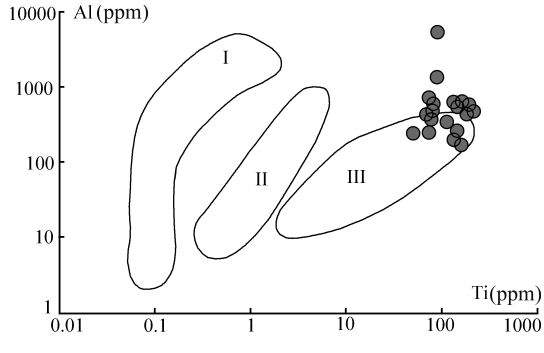

Fig. 4. Al-Ti diagram for quartz on the Vosnesensky deposit. Roman numerals denote the compositional deposits of ore quartz of epithermal (I), mesothermal orogenic gold ore (II) and porphyry (III) deposits (Rusk, 2012). Data for the Vosnesensky deposit are shown with gray circles.

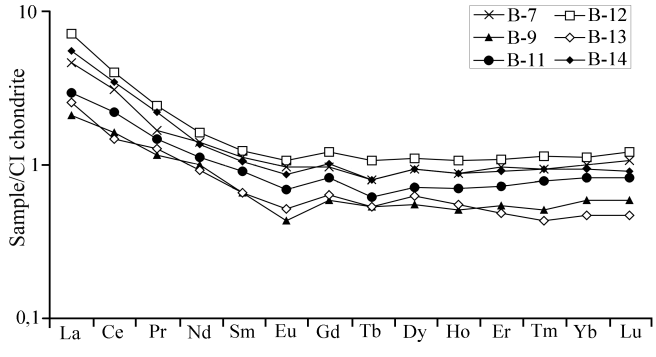

Fig. 5. Graphs of REE distribution in pyrite

indicate the crystallization of pyrite from a relatively oxidized fluid at low temperatures, apparently below 250°C (Bau, Möller, 1992).

Negative Ce anomalies could arise as a result of the interaction of fluid with marine limestones, which are present in the exocontact zones of the Vosnesensky massif. For marine limestones, negative Ce anomalies are characteristic, which persist during fluid/limestone interaction (Castorina, Masi, 2008). In addition, oxidized meteoric waters could have been involved in the ore-forming system of the deposit, which is indirectly indicated by a weak positive trend in the relationship between the homogenization temperatures of inclusions and the salinity of fluids (Wilkinson, 2001). The dilution of fluids with meteoric waters led to a drop in fluid temperatures and salinity.

The sources of ore-forming fluids can be judged by the value of the Y/Ho ratio in ore minerals (Bau, 1996). The Y/Ho values in the pyrite of the Vosnesensky deposit vary in the range 27.6–36.8. Some of these values fall within the range of Y/Ho values characteristic of ore-hosting granitoids (29.4–35.7), while others – for marine carbonates (Figure 6).

The results of the studies made it possible to assume the participation of a magmatic fluid in the ore-forming processes of the deposit and, like negative Ce anomalies, indicate its interaction with the host limestones. It should be noted that the distribution spectra of REE in pyrite are very close to the trends in the distribution of lanthanides in ore-bearing granitoids. Chondrite-normalized REE distribution spectra in granitoids of the deposit are also characterized by enrichment in light lanthanides (LaN/YbN = 1.5–6.0) and lack of differentiation among heavy rare earths (GdN/YbN = 0.83–1.07) (Znamensky et al., 2019). In our opinion, this can serve as an additional argument in favor of the magmatogenic nature of the ore-forming fluid. The participation of magmatogenic fluids in ore formation is confirmed by the results of S isotope analysis in sulfides. The $\delta^{34}S$ values, which are –1.01 ... 0.8 ‰ in pyrite and 0.9 ‰ in chalcopyrite, are close to the meteorite standard. The obtained $\delta^{34}S$ values correspond to the isotopic ratios of sulfur in sulfides of most porphyry deposits in the Southern Urals, as well as in North and South America (0 ± 5 ‰) (Grabezhev, 2009; Ohmoto, Rye, 1979; Ohmoto, Goldhaber, 1997).

Thus, the porphyry Cu mineralization of the Vosnesensky deposit was formed under mesothermal conditions with the participation of acidic K-Na aqueous chloride fluids of magmatic nature, enriched in aluminum and light rare earth elements. The reduction in temperature and salinity of the fluid is due to its dilution by meteoric waters. Geochemical signs of the interaction of the fluid with the host limestones, expressed in negative Ce anomalies and increased values of the Y/Ho coefficient in ore pyrite, have been established.

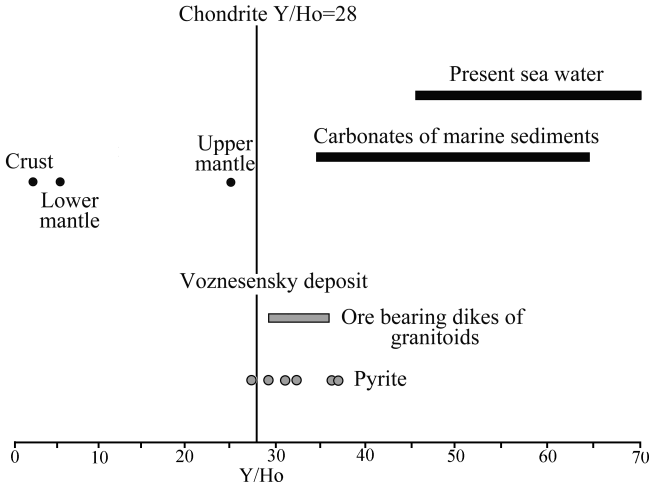

Fig. 6. The magnitude of the Y/Ho ratio in pyrite. Y/Ho values in chondrite, crust, upper and lower mantle, sea water, and carbonates of marine sediments according to (Bau, 1996; Bau, Dulski, 1995), in ore bearing dikes of the Vosnesensky deposit granitoids according to (Znamensky et al., 2019).

Acknowledgements

Field works were carried out under the Government Order of the Institute of Geology of the UFRC RAS No. 0246-2019-0078. Isotope and geochemical studies were supported by the RFBR (No. 17-45-020717). Fluid inclusion and LA-ICP-MS studies were supported by the State Contract of the Institute of Mineralogy SU FRC MG UB RAS (2019-21).

References

Abramov S.S.,Plotinskaya O.YU. Groznova Ye.O. (2016). History of hydrothermal processes at the Mikheevsky Mo-Cu field according to the study of secondary changes and fluid inclusions. Proc. XVII All-Russ. Conf. on Thermobaric geochemistry. Ulan-Ude: BNTS SO RAN, pp. 11–12. (In Russ.).

Bau M. (1996). Controls on the fractionation of isovalent trace elements in magmatic and agueous systems: evidence from Y/Ho, Zr/Hf and lanthanide tetrad effect. *Contrib. Mineral. Petrol*., 123, pp. 323–333. https://doi.org/10.1007/s004100050159

Bau M., Dulski, P. (1995). Comparative study of yttrium and rare-earth element behaviours in fluorine-rich hydrothermal fluids. *Contrib. Mineral. Petrol*, 119, pp. 213–223. https://doi.org/10.1007/BF00307282

Bau M., Möller P. (1992). Rare Earth Element Fractionation in Metamorphogenic Hydrothermal Calcite, Magnesite and Siderite. *Mineralogy and Petrology*, 45, pp. 231–246. https://doi.org/10.1007/BF01163114

Bodnar R.J., Vityk M.O. (1994). Interpretation of microthermometric data for H_2O-NaCl fluid inclusions. Fluid inclusions in minerals: methods and applications (Eds. De Vivo B. and Frezzotti M.L). Pontignana-Siena, Virginia Polytechnic Institute and State University, 1994, pp. 117–130.

Castorina F., Masi U. (2008). REE and Nd-isotope evidence for the origin siderite from the Jebel Awam deposit (Central Morocco). *Ore Geology Reviews*, 34, pp. 337–342. https://doi.org/10.1016/j.oregeorev.2008.03.001

Davis D.W., Lowenstein T.K., Spenser R.J. (1990). Melting behavior of fluid inclusions in laboratory-grown halite crystals in the systems NaCl-H_2O, NaCl-KCl-H_2O, NaCl-$MgCl_2$-H_2O and $CaCl_2$-NaCl-H_2O. *Geochim. Et Cosmochim. Acta*, 54, pp. 591–601. https://doi.org/10.1016/0016-7037(90)90355-O

Grabezhev A.I. (2009). Sr-Nd-C-O-H-S isotope-geochemical description of South Urals porphyry-copper fluid-magmatic systems: probable sources of matter. *Litosfera*, 6, pp. 66–89. (In Russ.)

Grabezhev A.I., Belgorodsky E.A. (1992). Productive granites and metasomatites of copper-porphyry deposits. Ekaterinburg: Nauka, 199 p. (In Russ.)

Guangzhou M., Renmin H., Jianfeng G., Weiqiang L., Kuidong Z., Guangming L.(2009). Existing forms of REE in gold-bearing pyrite of the Jinshan gold deposit, Jiangxi Province, China. *Journal of rare earths*, 27(6), pp. 1079–1087. https://doi.org/10.1016/S1002-0721(08)60392-0

Kosarev A.M., Puchkov V.N., Seravkin I.B., Kholodnov V.V., Grabezhtv A.I., Ronkin Y.L. (2014). New data on the age and geodynamic position of copper-porphyry mineralization in the Main Uralian Fault zone (Southern Urals). *Doklady Earth Sciences,* 495(1), pp. 1317–1321. https://doi.org/10.1134/S1028334X1411004X

McDonough W. F., Sun S. (1995). The composition of the Earth. *Chemical Geology*, 120, pp. 223–253. https://doi.org/10.1016/0009-2541(94)00140-4

Ohmoto H., Rye R. O. (1979). Isotopes of sulfur and carbon. *Geochemistry of hydrothermal ore deposits*. N.-Y.: John Wiley and Sons, pp. 509–567.

Ohmoto H., Goldhaber M. B. (1997). Sulfur and carbon isotopes. *Geochemistry of hydrothermal ore deposits*. N.-Y.: Wiley, pp. 517–611.

Prokofev V.Y., Afanaseva Z.B., Ivanova G.F., Boiron M.C., Marignac C. (1994). Study of fluid inclusions in minerals of the Olimpiadinskoe Au (Sb-W) deposit (Enisey Mountain-Ridge). *Geokhimiya,* pp. 1012-1029. (In Russ.)

Rimskaya-Korsakova M.N., Dubinin A.V. (2003). Rare earth elements in sulfides of submarine hydrothermal vents of the Atlantic ocean. *Doklady Earth Sciences,* 389(3), pp. 432–436.

Roedder E. (1984). Fluid inclusions. *Reviews in mineralogy,* 12, 646 p.

Rusk B.G. (2012). Cathodoluminescent textures and trace elements in hydrothermal quartz. Quartz: Deposits, Mineralogy and Analytics. New-York: Springer, 360 p. https://doi.org/10.1007/978-3-642-22161-3_14

Rusk B.G., Lowers H.A., Reed M.H. (2008). Trace elements in hydrothermal quartz: Relationships to cathodoluminescent textures and insights into vein formation. *Geology*, 36(7), pp. 547–550. https://doi.org/10.1130/G24580A.1

Schwim G., Markl G. (2005). REE systimatics in hydrothermal fluorite. *Chemical Geology*, 216, pp. 225–248. https://doi.org/10.1016/j.chemgeo.2004.11.012

Shishakov V.B., Sergeeva N.E., Surin S.V. (1988). The Voznesenskoe porphyry copper deposit at South Urals. *Geologiya rudnykh mestorozhdeniy,* 2, pp. 85–90. (In Russ.)

Sverjensky D.A. (1984). Europium redox equilibria in aqueous solution. *Earth Planet Science Letters*, 67, pp. 70–78.

Wilkinson J.J. (2001). Fluid inclusions in hydrothermal ore deposits. *Lithos*, 55, pp. 229–272. https://doi.org/10.1016/S0024-4937(00)00047-5

Znamensky S.E. (2017). Rare earth elements and yttrium in calcite and pyrite of the Orlovka gold deposit (the Southern Urals). *LITHOSPHERE (Russia)*, 1, pp. 135–146. (In Russ.)

Znamensky S.E., Shafigullina G.T., Znamenskaya N.M., Kosarev A.M. (2019). The Voznesenka porphyry copper deposit (South Urals): structural control of mineralization and geochemistry of intrusive rocks. *Vestnik Akademii nauk Respubliki Bashkortostan*, 2, pp. 25–35 (In Russ.)

About the Authors

Sergey E. Znamensky – Dr. Sci. (Geology and Mineralogy), Chief Researcher, Institute of Geology of the Ufa Federal Research Centre of the Russian Academy of Sciences

16/2 K. Marx st., Ufa, 450077, Russian Federation

Natalya N. Ankusheva – Cand. Sci. (Geology and Mineralogy), Researcher, Institute of Mineralogy of the South Urals Federal Research Center of Mineralogy and Geoecology of the Urals Branch of the Russian Academy of Sciences

1 Ilmensky Zapovednik, Miass, 456317, Russian Federation

Dmitry A. Artemiev – Cand. Sci. (Geology and Mineralogy), Researcher, Institute of Mineralogy of the South Urals Federal Research Center of Mineralogy and Geoecology of the Urals Branch of the Russian Academy of Sciences

1 Ilmensky Zapovednik, Miass, 456317, Russian Federation

Manuscript received 9 January 2020;
Accepted 11 June 2020; Published 30 September 2020